

APPENDIX

The effect of COVID-19 vaccination in Italy and perspectives for “living with the virus”

Valentina Marziano ^{1,2,#}, Giorgio Guzzetta ^{1,2,#}, Alessia Mammone ³, Flavia Riccardo ⁴, Piero Poletti ^{1,2}, Filippo Trentini ^{1,2}, Mattia Manica ^{1,2}, Andrea Siddu ³, Antonino Bella ⁴, Paola Stefanelli ⁴, Patrizio Pezzotti ⁴, Marco Ajelli ^{5,6,^}, Silvio Brusaferrò ^{4,^}, Giovanni Rezza ^{3,^}, Stefano Merler ^{1,2,^,*}

Affiliations:

¹ Center for Health Emergencies, Bruno Kessler Foundation, Trento, Italy

² Epilab-JRU, FEM-FBK Joint Research Unit, Trento, Italy

³ Health Prevention, Ministry of Health, Rome, Italy

⁴ Istituto Superiore di Sanità, Rome, Italy

⁵ Laboratory for Computational Epidemiology and Public Health, Indiana University School of Public Health, Bloomington, United States

⁶ Laboratory for the Modeling of Biological and Socio-technical Systems, Northeastern University, Boston, United States

joint first authors

^ joint senior authors

* corresponding author: Stefano Merler, merler@fbk.eu

Contents

The effect of COVID-19 vaccination in Italy and perspectives for “living with the virus”	1
1. Materials and Methods.....	2
1.1 Model for SARS-CoV-2 transmission and vaccination	2
1.2 Reproducing the SARS-CoV-2 epidemic trajectory in Italy	4
1.3 Model initialization	5
1.4 Computation of age-specific vaccination rates over time.....	7
1.5 Vaccine efficacy against infection and death	8
1.6 Model outputs	9
1.7 No vaccination scenario	10
1.8 Future vaccination scenarios for the Delta variant	10
2. Sensitivity analyses.....	12
2.1 Description	12
2.2 Results.....	13
References	16

37 1. Materials and Methods

38 1.1 Model for SARS-CoV-2 transmission and vaccination

39 We developed an age-structured stochastic model for SARS-CoV-2 transmission and vaccination, based on a
40 susceptible-infectious-removed-susceptible scheme (SIRS) and adapted from previously published models [1,2].
41 Mixing patterns are assumed to be heterogeneous across ages according to an age-specific social contact matrix
42 estimated prior to the COVID-19 pandemic [3]. We assume an age-dependent susceptibility to SARS-CoV-2
43 infection: lower in children under 15 years of age and higher for the elderly (65+), compared to individuals of
44 working age [4].

45 We simulate a two-dose vaccination campaign. In the baseline analysis, vaccination is assumed to reduce the
46 individuals' susceptibility to SARS-CoV-2 infection and the risk of death. Breakthrough infections (i.e., infections
47 in vaccinated individuals) are assumed to be half as infectious as those in unvaccinated individuals [5,6]. The
48 model accounts for waning of both natural and vaccine-induced protection, where the duration is exponentially
49 distributed (mean: 2 years [7,8]). Specifically, before waning of natural immunity individuals are fully protected
50 against infection; while before waning of vaccine protection, vaccine reduces the probability of infection and
51 death (with different efficacy estimates for the two endpoints) and the infectiousness of breakthrough
52 infections. After waning of either natural or vaccine protection, individuals are considered fully susceptible.
53 Alternative durations for natural immunity and vaccine protection are explored as sensitivity analyses (1 year
54 and 10 years), as well as the case of a vaccine not reducing infectiousness (see Section 2.1). Immunity gained
55 after experiencing both vaccination and infection (independently of the order) is assumed not to wane over the
56 time scale of our simulations.

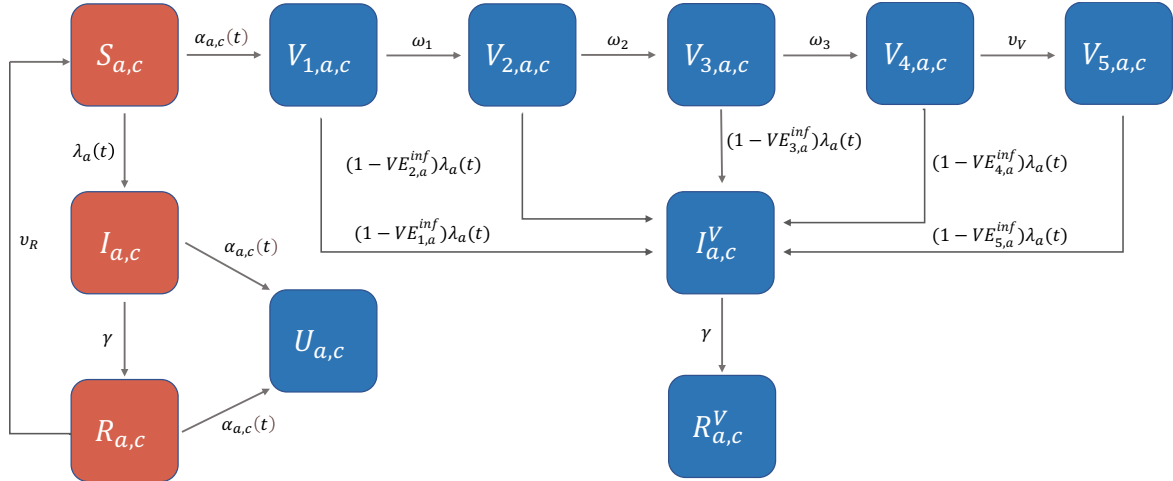
57 The baseline model is described by the following system of differential equations (summarized by the schematic
58 representation in Figure S1):

$$59 \left\{ \begin{array}{l} S'_{a,c}(t) = -\lambda_a(t)S_{a,c}(t) - \alpha_{a,c}(t)S_{a,c}(t) + v_N R_{a,c}(t) \\ I'_{a,c}(t) = \lambda_a(t)S_{a,c}(t) - \gamma I_{a,c}(t) - \alpha_{a,c}(t)I_{a,c}(t) \\ R'_{a,c}(t) = \gamma I_{a,c}(t) - \alpha_{a,c}(t)R_{a,c}(t) - v_N R_{a,c}(t) \\ U'_{a,c}(t) = \alpha_{a,c}(t)(I_{a,c}(t) + R_{a,c}(t)) \\ V'_{1,a,c}(t) = \alpha_{a,c}(t)S_{a,c}(t) - (1 - VE_{1,a}^{inf})\lambda_a(t)V_{1,a,c} - \omega_0 V_{1,a,c}(t) \\ V'_{2,a,c}(t) = \omega_0 V_{1,a,c}(t) - (1 - VE_{2,a}^{inf})\lambda_a(t)V_{2,a,c} - \omega_1 V_{2,a,c}(t) \\ V'_{3,a,c}(t) = \omega_1 V_{2,a,c}(t) - (1 - VE_{3,a}^{inf})\lambda_a(t)V_{3,a,c} - \omega_2 V_{3,a,c}(t) \\ V'_{4,a,c}(t) = \omega_2 V_{3,a,c}(t) - (1 - VE_{4,a}^{inf})\lambda_a(t)V_{4,a,c} - v_V V_{4,a,c}(t) \\ V'_{5,a,c}(t) = v_V V_{4,a,c}(t) - (1 - VE_{5,a}^{inf})\lambda_a(t)V_{5,a,c}(t) \\ I_{a,c}^V(t) = \lambda_a(t)[(1 - VE_{1,a}^{inf})V_{1,a,c} + (1 - VE_{2,a}^{inf})V_{2,a,c} + (1 - VE_{3,a}^{inf})V_{3,a,c} + (1 - VE_{4,a}^{inf})V_{4,a,c} + (1 - VE_{5,a}^{inf})V_{5,a,c}(t)] - \gamma I_{a,c}^V(t) \\ R'_{a,c}(t) = \gamma I_{a,c}^V(t) \end{array} \right.$$

60 where:

- 61 • the population class $\{a,c\}$ represents individuals in age group a and in underlying conditions status c
62 (“with” or “without”);
- 63 • $S_{a,c}$ represents the number of unvaccinated individuals in the population class $\{a,c\}$ who are fully
64 susceptible to SARS-CoV-2 infection;
- 65 • $I_{a,c}$ represents the number of infectious unvaccinated individuals in the population class $\{a,c\}$.
- 66 • $R_{a,c}$ represents the number of unvaccinated individuals in the population class $\{a,c\}$ who recovered
67 from infection.
- 68 • $U_{a,c}$ represents the number of individuals in the population class $\{a,c\}$ who are vaccinated despite
69 having already experienced SARS-CoV-2 infection.
- 70 • $V_{1,a,c}; V_{2,a,c}; V_{3,a,c}; V_{4,a,c}$ and $V_{5,a,c}$ represent the number of vaccinated individuals at different stages of
71 protection. In particular,
72 1) $V_{1,a,c}$ denotes individuals in the population class $\{a,c\}$ vaccinated with the first dose, for whom
73 the first dose is not effective yet.
74 2) $V_{2,a,c}$ denotes individuals in the population class $\{a,c\}$ vaccinated with the first dose, for whom
75 the first dose is effective.
76 3) $V_{3,a,c}$ denotes individuals in the population class $\{a,c\}$ vaccinated with the second dose for
77 whom the second dose is not effective yet.

- 78 4) $V_{4,a,c}$ denotes individuals in the population class $\{a,c\}$ vaccinated with the second dose for
 79 whom the second dose is effective.
 80 5) $V_{5,a,c}$ denotes individuals in the population class $\{a,c\}$ vaccinated with the second dose for
 81 whom vaccine protection has waned.
 82 • $I_{a,c}^V$ represents the number of infectious individuals in the population class $\{a,c\}$ among those who have
 83 already received at least one vaccine dose.
 84 • $R_{a,c}^V$ represents the number of individuals in the population class $\{a,c\}$ who recovered from an infection
 85 contracted after having received at least one vaccine dose.



86 **Figure S1. Schematic representation of the baseline model.** Red compartments represent unvaccinated individuals and
 87 therefore eligible for vaccination; blue compartments represent vaccinated individuals. Model parameters include: the time-
 88 and age-dependent force of infection $\lambda_a(t)$; the recovery rate from infection (γ); the duration of immunity after infection
 89 ($1/v_R$); the time-, age- and group-dependent vaccination rate $\alpha_{a,c}(t)$; the average interval between administration of the
 90 first dose and full protection by the first dose ($1/\omega_1$); the average interval between full protection of the first dose and
 91 administration of the second dose ($1/\omega_2$); the average interval between administration of the second dose and full
 92 protection of the 2nd dose ($1/\omega_3$); the average duration of vaccine protection after administration of the second dose
 93 ($1/v_V$); age-dependent vaccine efficacies against infection in the different stages i of vaccine protection ($i=1,2,3,4,5$) are
 94 denoted by $VE_{i,a}^{inf}$.
 95

96 Susceptible individuals are exposed to a time and age-dependent force of infection $\lambda_a(t)$ which is defined as:

$$97 \quad \lambda_a(t) = \beta(1 + \theta_{\text{Alpha}})(1 - \varphi) \delta(t) r_a \sum_{\tilde{a}} C_{a,\tilde{a}} \frac{\sum_c [I_{\tilde{a},c}(t) + \pi I_{\tilde{a},c}^V(t)]}{\sum_c N_{\tilde{a},c}}$$

98 where:

- 99 • β is a scaling factor shaping SARS-CoV-2 transmissibility in the absence of physical distancing
 100 restrictions (PDRs) and other non-pharmaceutical interventions (NPIs) such as face masks or hand
 101 hygiene precautions, computed by assuming $R_0=3.0$, as estimated for historical lineages of SARS-CoV-2
 102 in Italy [9,10,11].
 103 • θ_{Alpha} is a coefficient representing the transmissibility increase of the Alpha variant with respect to
 104 historical lineages. We assumed $\theta_{\text{Alpha}} = 0.5$ [12-16].
 105 • $(1 - \varphi)$ is a coefficient representing the reduction in the per-contact transmission probability
 106 ascribable to preventive transmission measures such as face masks or hand hygiene precautions. We
 107 assumed $\varphi = 20\%$ [9,10].
 108 • $\delta(t) \in \{0,1\}$ is a scaling factor representing the proportion of pre-pandemic contacts that are active at
 109 time t .
 110 • r_a is the relative susceptibility to SARS-CoV-2 infection at age a . We sample susceptibility profiles from
 111 the posterior distribution estimated in [4], having mean values $r_a=0.58$ (95%CI 0.34-0.98) under 15
 112 years of age; $r_a=1$ between 15 and 64 years; and $r_a=1.65$ (95%CI 1.03-2.65) above 64 years.
 113 • $C_{a,\tilde{a}}$ represents the age-group-specific contact matrix, as estimated before the SARS-CoV-2 pandemic
 114 [3], whose entries describe the mean numbers of persons in age group \tilde{a} encountered by an individual
 115 of age group a in an average day.

116 • π represents the relative infectiousness of SARS-CoV-2 cases among vaccinated compared to
 117 unvaccinated. We assumed $\pi = 0.5$ [5,6].

118 • $N_{\tilde{a},c}$ represents the number of individuals in the population class $\{\tilde{a},c\}$.

119 For all infectious compartments, the average duration of infectiousness ($1/\gamma$) is set equal to the average
 120 generation time (6.6 days) [9]. The model described by the system of ordinary differential equations above is
 121 implemented through a stochastic discrete-time model with a time step $\tau = \frac{1}{4}$ day.

122 At each time t , the number of unvaccinated individuals in the population class $\{a,c\}$ (red compartments in Figure
 123 S1) who will receive a first vaccine dose is determined as a fraction $z_{a,c}(t)$ of the corresponding population:

$$124 \quad z_{a,c}(t) = \frac{d_{a,c}(t)}{S_{a,c}(t) + I_{a,c}(t) + R_{a,c}(t)}$$

125 where $d_{a,c}(t)$ represents the number of first vaccine doses administered to individuals of the population class
 126 $\{a,c\}$ at time t . The value of $d_{a,c}(t)$ is inferred from data on the daily number of first doses administered by age
 127 group in Italy between the start of vaccination (December 27, 2020) and the end of the simulated period (June
 128 30, 2021) [17]. Details are reported in Section 1.4.

129 The vaccination rate $\alpha_{a,c}(t)$ associated to the probability $z_{a,c}(t)$ in the differential equations model can be
 130 computed through the following equation

$$131 \quad z_{a,c}(t) = 1 - e^{-\alpha_{a,c}(t)\tau}.$$

132 We assume that the first dose becomes effective on average after $1/\omega_1 = 14$ days from its administration [18],
 133 that the second dose is administered on average 42 days after the first dose (i.e. $1/\omega_1 + 1/\omega_2 = 42$ days and
 134 $1/\omega_2 = 28$ days) [19,20], and that the 2nd dose becomes effective after $1/\omega_3 = 7$ days from its administration
 135 [18]. In the baseline analysis, we assume that the protection gained after both infection and completion of the
 136 vaccination schedule lasts on average two years, i.e. $1/v_R = 1/v_V = 730$ days [7,8].

137 Vaccinated individuals $V_{i,a,c}$ at any stage of protection i can develop breakthrough infection with a susceptibility
 138 reduced by a factor $1 - VE_{i,a}^{inf}$, where $VE_{i,a}^{inf}$ represents the age-specific vaccine efficacy associated to the i -th
 139 stage of protection. We assume that the vaccine efficacy is the same in individuals with and without
 140 comorbidities. Vaccinated individuals for whom vaccine protection has waned ($V_{5,a,c}$) are fully susceptible to
 141 infection as unvaccinated individuals (i.e. $VE_{5,a}^{inf} = 0$ for all ages a). Details on the age-specific vaccine efficacy
 142 against infection are reported in Section 1.5.

144 1.2 Reproducing the SARS-CoV-2 epidemic trajectory in Italy

145 The reproduction number associated to the dynamical system considered can be computed as the dominant
 146 eigenvalue of the Next Generation Matrix (NGM) [21,22,23], defined as:

$$147 \quad NGM = \frac{\beta(1 + \theta_{Alpha})(1 - \varphi) \delta(t)}{\gamma} \begin{pmatrix} B_{a,\tilde{a}}^{V_0,IV_0} & B_{a,\tilde{a}}^{V_0,IV_1} & B_{a,\tilde{a}}^{V_0,IV_2} & B_{a,\tilde{a}}^{V_0,IV_3} & B_{a,\tilde{a}}^{V_0,IV_4} & B_{a,\tilde{a}}^{V_0,IV_5} \\ B_{a,\tilde{a}}^{V_1,IV_0} & B_{a,\tilde{a}}^{V_1,IV_1} & B_{a,\tilde{a}}^{V_1,IV_2} & B_{a,\tilde{a}}^{V_1,IV_3} & B_{a,\tilde{a}}^{V_1,IV_4} & B_{a,\tilde{a}}^{V_1,IV_5} \\ B_{a,\tilde{a}}^{V_2,IV_0} & B_{a,\tilde{a}}^{V_2,IV_1} & B_{a,\tilde{a}}^{V_2,IV_2} & B_{a,\tilde{a}}^{V_2,IV_3} & B_{a,\tilde{a}}^{V_2,IV_4} & B_{a,\tilde{a}}^{V_2,IV_5} \\ B_{a,\tilde{a}}^{V_3,IV_0} & B_{a,\tilde{a}}^{V_3,IV_1} & B_{a,\tilde{a}}^{V_3,IV_2} & B_{a,\tilde{a}}^{V_3,IV_3} & B_{a,\tilde{a}}^{V_3,IV_4} & B_{a,\tilde{a}}^{V_3,IV_5} \\ B_{a,\tilde{a}}^{V_4,IV_0} & B_{a,\tilde{a}}^{V_4,IV_1} & B_{a,\tilde{a}}^{V_4,IV_2} & B_{a,\tilde{a}}^{V_4,IV_3} & B_{a,\tilde{a}}^{V_4,IV_4} & B_{a,\tilde{a}}^{V_4,IV_5} \\ B_{a,\tilde{a}}^{V_5,IV_0} & B_{a,\tilde{a}}^{V_5,IV_1} & B_{a,\tilde{a}}^{V_5,IV_2} & B_{a,\tilde{a}}^{V_5,IV_3} & B_{a,\tilde{a}}^{V_5,IV_4} & B_{a,\tilde{a}}^{V_5,IV_5} \end{pmatrix} \quad (1)$$

148

149 Each block $B_{a,\tilde{a}}^{V_i,IV_j}$ describes the contribution to the transmission of age-specific interactions between
 150 susceptible individuals in compartment V_i and infectious individuals in the compartment IV_j , where $IV_j = I$ for
 151 $j=0$, while IV_j represents individuals infected in the j -stage of vaccine protection for $j>0$. For simplicity, we
 152 denote here the class of unvaccinated individuals with V_0 , while V_1, V_2, V_3, V_4 and V_5 denote vaccinated
 153 individuals in the different stages of vaccine protection.

154 Specifically, the explicit computation of the NGM starting from model equations yields:

155

$$B_{a,\tilde{a}}^{V_i V_j} = r_a C_{a,\tilde{a}} [1 - VE_{i,a}^{inf}] \chi_{IV_j} \frac{N_{\tilde{a}}^{V_j}(t)}{N_{\tilde{a}}}$$

156 where:

157

- $VE_{i,a}^{inf}$ is the vaccine efficacy against infection for individuals of age a with vaccination status V_i (with $VE_{0,a}^{inf} = 0$ by definition).

158

159

- χ_{IV_j} is the relative infectiousness of SARS-CoV-2 cases among vaccinated compared to unvaccinated (equal to π for vaccinated compartments, and 1 for the unvaccinated).

160

161

- $N_{\tilde{a}}^{V_j}(t)$ is the number of individuals of age \tilde{a} with vaccination status V_j at time t

162

- $N_{\tilde{a}}$ represents the total population of age \tilde{a} .

163

The distribution of the scaling factor shaping SARS-CoV-2 transmissibility for historical lineages (β) under full resumption of pre-pandemic contacts ($\delta(t) = 1$) and in the absence of preventive measures ($\varphi = 0$), can be computed analytically from Equation 1 given the distribution of the age-specific susceptibility profile (r_a), the distribution of the bootstrapped contact matrix ($C_{a,\tilde{a}}$), the value of γ , the value of θ_{Alpha} , and assuming $R_0 = 3.0$, as estimated in Italy in the early phase of the pandemic [9,10].

168

To reproduce the epidemic trajectory observed in Italy between January and June 2021 we use Equation 1 to recalibrate at each time step ($\tau = \frac{1}{4} day$) the value of $\delta(t)$. In particular, the selected value of $\delta(t)$ will be the one that will make the model's reproduction number (recomputed after updating the $N_{\tilde{a}}^{V_j}(t)$ to current state variables of the model) match the corresponding value of the net reproduction number as estimated on the same day from epidemic curves collected by the national integrated surveillance system [10,24] (reported in Figure S2).

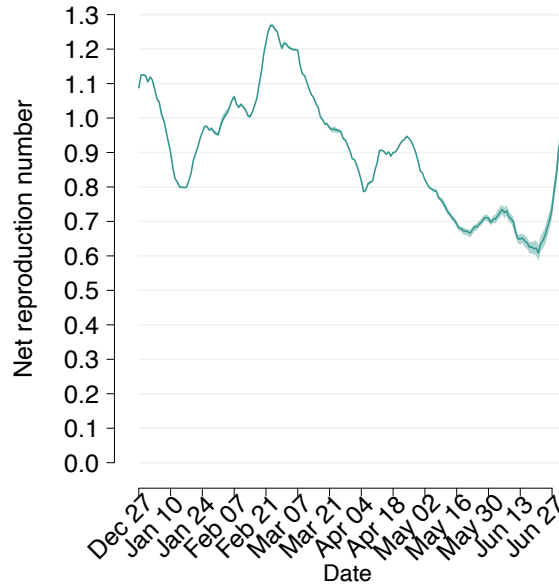
169

170

171

172

173



174

Figure S2. Estimates of the net reproduction number R_t the net reproduction number as obtained from epidemic curves collected by the National Integrated Surveillance System [24]

175

176

Results discussed in the main text and in the following sections were obtained by running 300 simulations, sampling at each run a different value from the joint distribution of the transmission coefficient β , the bootstrapped contact matrices $C_{a,\tilde{a}}$ and the relative susceptibility by age r_a .

177

178

179

180 1.3 Model initialization

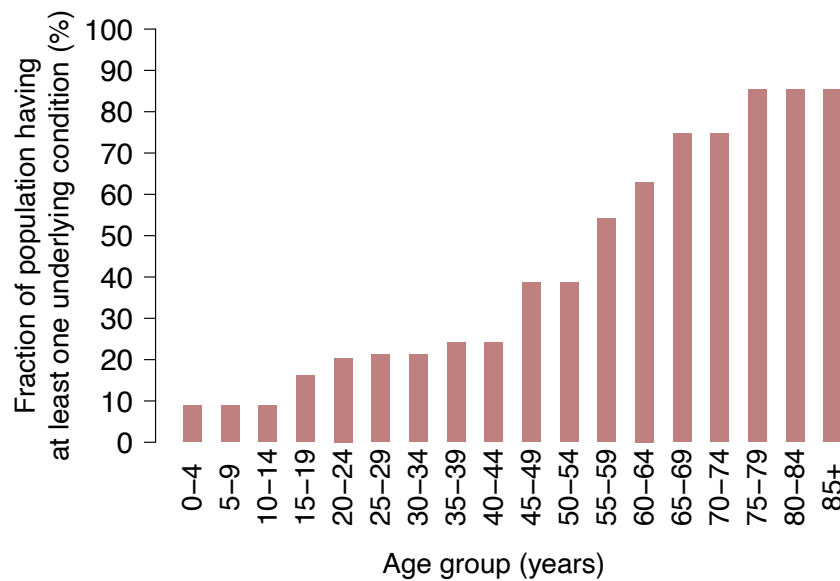
181

The model is used to simulate SARS-CoV-2 infection and vaccination dynamics in Italy between the start of the vaccination campaign (December 27, 2020) and June 30, 2021.

182

183 The population by age was initialized according to the Italian age structure in 2020 [25] and statistics on
 184 underlying conditions, among which chronic respiratory disease, cardio-cerebrovascular disease, hypertension
 185 and diabetes [26] (Figure S3).

186



187

188 **Figure S3. Fraction of the population having at least one underlying condition by age (%) [26]**

189 **Fraction of initially immune individuals.** The spread of SARS-CoV-2 in Italy throughout 2020 has been
 190 characterized by marked regional heterogeneities and estimates for the fraction of immune population in Italy
 191 by the end of December 2020 are not available. We considered three different Italian regions, that are
 192 representative of different levels of SARS-CoV-2 circulation:

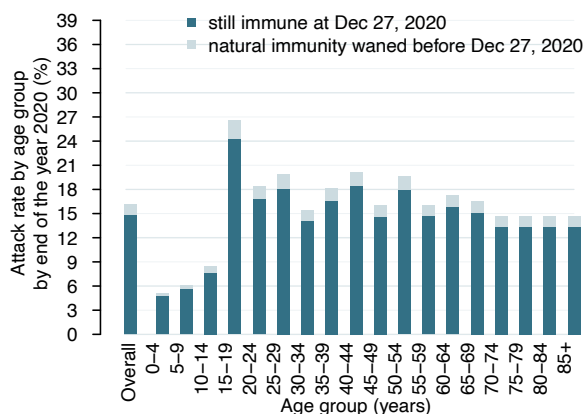
- 193 • Lombardy, the first and hardest hit region in 2020;
- 194 • Lazio, characterized by an intermediate circulation of SARS-CoV-2 in 2020;
- 195 • Campania, characterized by low circulation of SARS-CoV-2 in 2020.

196 For each region, we adapted a previously published model [1] to obtain estimates of the age-specific fraction of
 197 individuals infected with SARS-CoV-2 by December 27, 2020. Estimates obtained for Lazio were used to initialize
 198 the fraction of recovered population at the national level in the baseline analysis (“intermediate” immunity
 199 scenario), and those obtained for the two other regions were used in sensitivity analyses (“low” immunity:
 200 Campania; “high” immunity: Lombardy). For the baseline analysis (intermediate scenario), we obtained that
 201 about 16% of the overall population was infected with SARS-CoV-2 prior to the introduction of vaccination
 202 (Figure S4), while for the low and high immunity scenarios these fractions are 9% and 23%, respectively (Figure
 203 S5).

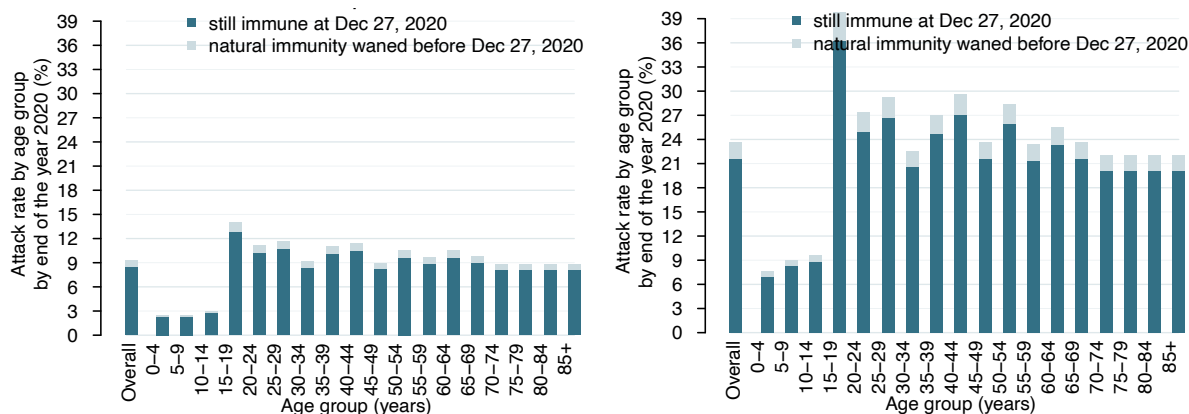
204 Under the assumption of natural immunity lasting on average $1/v_R$, we estimated the proportion f of recovered
 205 individuals that would have lost natural immunity by December 27, 2020. To this aim, we consider the time
 206 series of daily SARS-CoV-2 cases notified in Italy throughout 2020 [27] and, for each individual case i notified on
 207 day t , we determined if his/her natural immunity has waned by sampling the duration from an exponential
 208 distribution with average $1/v_R$.

209 Assuming a baseline average value for the duration of natural immunity of 2 years, we obtained that a fraction
 210 $f=8.9\%$ of individuals recovered from SARS-CoV-2 by the end of 2020 may have lost natural immunity by that
 211 time (light blue in Figure S4-S5).

212



213 **Figure S4. Intermediate immunity scenario.** Overall and age-specific fraction of population with natural immunity to SARS-
 214 CoV-2 in the intermediate immunity scenario at the beginning of the vaccination campaign [1].
 215
 216
 217



218 **Figure S5. Low and high immunity scenarios.** Left: Overall and age-specific fraction of population with natural immunity to
 219 SARS-CoV-2 in the low immunity scenario at the beginning of the vaccination campaign [1]. Right: The same as left, but for
 220 the high immunity scenario.
 221
 222

223 **Initially infectious individuals.** The number of infected individuals at the beginning of simulations (December 27,
 224 2020) was determined in such a way to match the average daily number of notified cases reported in the week
 225 of simulations start (around 15,000) [27]. The reporting rate ρ for SARS-CoV-2 infections at the end of 2020 was
 226 estimated as

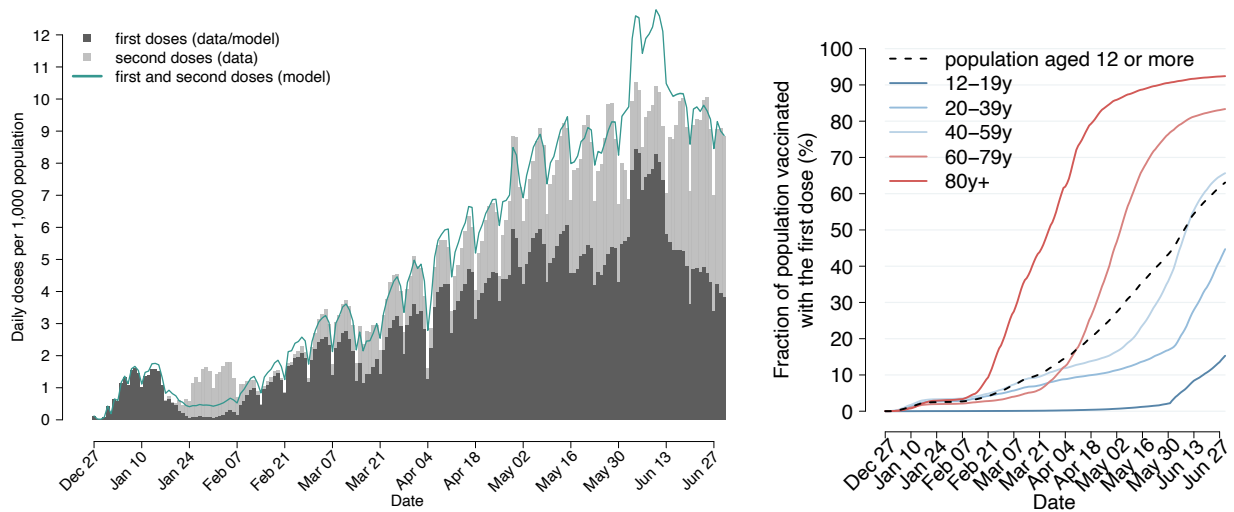
$$\rho = \varepsilon / CFR$$

227
 228 where ε is the infection fatality ratio estimated for Italy [28] and CFR is the case fatality ratio among SARS-CoV-2
 229 cases reported in the last three weeks of December, assuming a delay between diagnosis and death of about 3
 230 weeks [29]; thus, $CFR = M / C$ where C is the cumulative number of cases reported in the last 3 weeks of
 231 December 2020 and M represents the number of deaths reported in the first 3 weeks of January 2021 [30]. The
 232 resulting value for the reporting rate is 41.2%.

233 1.4 Computation of age-specific vaccination rates over time

234 The rollout of the two-dose vaccination campaign is modeled using detailed data on the daily age-specific
 235 number of first doses administered over the considered period [17]. In the model, second doses are assumed to
 236 be administered to all individuals who have been vaccinated with one dose after an average of 42 days since the
 237 first dose. As shown in Figure S6, the model well reproduces the observed scale-up of the daily vaccination
 238 capacity occurred in Italy in the first half of the year 2021. The priority order of the Italian vaccination campaign
 239 was based on the WHO SAGE roadmap [31, 32] prioritizing high-risk population age segments, i.e. over 80 years
 240 of age and essential workers (e.g. health care workers and teachers) and then progressively targeting younger
 241 age groups. In the absence of data regarding the presence or absence of underlying conditions in individuals
 242 targeted by vaccination, we assumed to distribute the daily doses proportionally to the prevalence of underlying

243 conditions in the age group considered. The evolution of vaccination coverage, by age and overall, as observed
 244 in the first half of the year 2021 is shown in Figure S6.
 245
 246
 247



248
 249 **Figure S6.** Left: daily vaccination capacity in Italy (number of doses per 1,000 population) as observed [17] (grey bars) and as
 250 estimated by the model (solid line) between December 27, 2020, and June 30, 2021. Right: first dose vaccination coverage
 251 overall (black dotted line) and by age group (solid lines) as observed in Italy between December 27, 2020, and January 30,
 252 2021 [17].
 253

254 1.5 Vaccine efficacy against infection and death

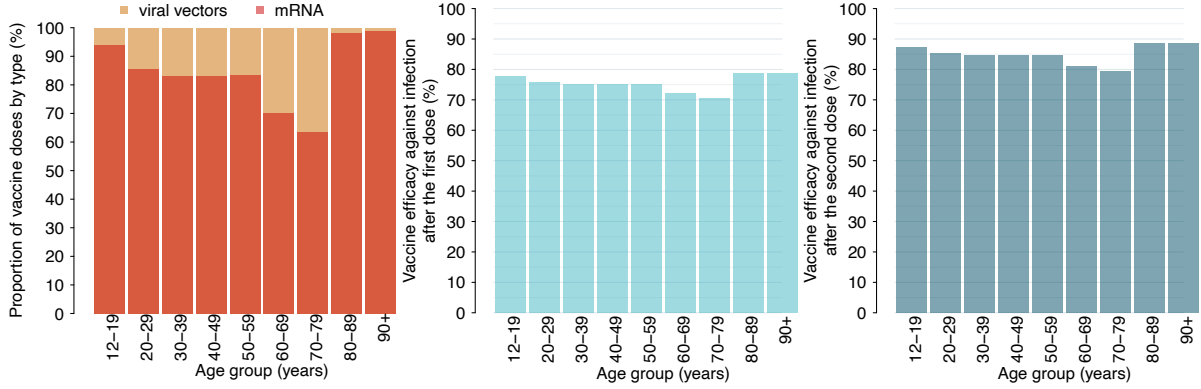
255 In the first half of 2021 about 51 million vaccine doses have been administered in Italy, about 71% of which
 256 were Pfizer- BioNTech, 17% AstraZeneca, 10% Moderna and 2% Janssen [17].
 257 Current evidence suggests an efficacy against infection with the Alpha variant of about 62% after two doses of
 258 AstraZeneca [33]. Estimates available for Pfizer-BioNTech suggest an efficacy against infection with Alpha of
 259 about 89% after two doses [34]. We inferred the corresponding vaccine efficacies after one dose of vaccine by
 260 assuming a 11% relative reduction compared to the efficacy observed after two doses [35, 36] (Table S1).

261 **Table S1.** Vaccine efficacy against symptomatic and asymptomatic infection

	1 DOSE	2 DOSES
Pfizer-BioNTech (mRNA)	79%*	89% [34]
AstraZeneca (viral vector)	55%*	62% [33]

*inferred

262
 263
 264 Using values reported in Table S1, we estimated an age-specific vaccine efficacy against infection by weighting
 265 the efficacy of a specific vaccine type (mRNA vs. viral vectors) by the number of vaccines of that type
 266 administered to each age group in the first half of 2021 [17] (Figure S7). We assume for the Moderna vaccine
 267 (mRNA type) the same vaccine efficacy of Pfizer-BioNTech and for Janssen (viral vector type) the vaccine same
 268 vaccine efficacy of AstraZeneca (Table S1). Obtained age-specific estimates are in good agreement with
 269 estimates obtained for Italy [37] and range between 70.6% and 78.8% after the first dose (average 75.5%) and
 270 between 79.4% and 88.7% after 2 doses (average: 84.9%).
 271



272
273
274
275
276

Figure S7. Left: Age-specific proportion of vaccine doses by vaccine type administered in the first half of 2021. mRNA vaccines administered in Italy include Pfizer-BioNTech and Moderna, while viral vector vaccines include AstraZeneca and Janssen. Center: Estimated age-specific vaccine efficacy against infection after the first dose (%). Right: Estimated age-specific vaccine efficacy against infection after the second dose (%).

277

278 Available estimates suggest a marked reduction in the risk of death in breakthrough infections: about 80.3% in
279 vaccinated with one dose and about 96.4% in vaccinated with two doses [37]. These values include the reduced
280 risk of SARS-CoV-2 infection in vaccinated compared to unvaccinated. To compute the infection fatality rate in
281 breakthrough infections at different stages of vaccine protection V_j , we estimate an age-specific scaling
282 coefficient $\mu_a^{V_j}$ representing the risk of death given SARS-CoV-2 breakthrough infection in each stage V_j relative
283 to infection in unvaccinated individuals:

284

$$\mu_a^{V_j} = \frac{1 - VE_{j,a}^{\text{inf}}}{1 - VE_j^{\text{death}}}$$

285
286

Where VE_j^{death} is set to 0 for unprotected individuals ($j=0, 1, 5$), to 80.3% for partially protected individuals ($j=2, 3$), and 96.4 for fully vaccinated individuals ($j=4$).

287

288 1.6 Model outputs

289 The main model outcomes are the age-specific number of new infections per day in the subpopulation $i_{a,c}^{V_j}(t)$ for
290 each vaccination stage j (including the unvaccinated, $j=0$); and the scaling factor $\delta(t)$ tuning the proportion of
291 pre-pandemic contacts necessary reproduce the daily official estimates of R_t .

292 Additional model outcomes are:

- 293 • the number of SARS-CoV-2 confirmed cases between December 27, 2020, and June 30, 2021 and
- 294 cumulative number of COVID-19 deaths over the same period;
- 295 • the immunity profile of the Italian population on June 30, 2021;
- 296 • estimates of the effective reproduction number (i.e., under the assumption of $\delta(t)=1$).

297

298 For each model outcome, we report the mean values and 95% confidence intervals across stochastic
299 simulations.

300

301 SARS-CoV-2 confirmed cases and COVID-19 deaths.

302 The daily number of SARS-CoV-2 confirmed cases is obtained from the daily infections by assuming a reporting
303 ratio (ρ) of 41.2% (see Section 1.3). The daily number of deaths in each subpopulation $\{a,c\}$ with vaccination
304 status V_j is obtained by applying the age-specific infection fatality ratio estimated for each population class ($\epsilon_{a,c}$)
305 to daily infections, considering a delay of 3 weeks (τ_D) between symptom onset and death [29], and rescaled by
306 a factor $(1 - q)$ to account for improvement in COVID-19 treatment. Specifically,

307

$$D_{a,c}^{V_j}(t) = \mu_a^{V_j} (1 - q) \epsilon_{a,c} i_{a,c}^{V_j}(t - \tau_D)$$

308
309
310

where $\mu_a^{V_j}$ is the relative risk of death in breakthrough infections, as computed in Section 1.5. To match the
cumulative number of deaths detected by the surveillance system over the considered period, we obtain a
reduction of mortality q by 20%.

311

The age-specific IFR for each population class ($\epsilon_{a,c}$) was estimated as:

$$\varepsilon_{a,c} = \psi_c \cdot \varepsilon_a = v \cdot \varepsilon_c \cdot \varepsilon_a$$

313 where

- 314 • ε_c denotes the overall IFR in class c , as estimated from Lombardy data [28].
- 315 • ε_a denotes the age-specific IFR as estimated independently of the presence of underlying conditions [28].
- 316 • the scale factor v is determined in such a way to minimize the root mean square error between ε_a and
- 317 $\bar{\varepsilon}_a = \sum_c P_{a,c} \cdot \varepsilon_{a,c}$, and $P_{a,c}$ denotes the proportions of individuals of age a in class c in the Italian
- 318 demographics [26].

319 Eventually, we obtain $\psi_{without}=0.20$ for individuals without underlying conditions and $\psi_{with}=1.16$ for

320 individuals with underlying conditions, consistent with the overall relative risk $\frac{\psi_{with}}{\psi_{without}} = 5.8$ estimated in [28].

321 **Effective reproduction number.** For each time t , the effective reproduction number is computed as the

322 dominant eigenvalue of the Next Generation Matrix defined in Equation (1) by setting $\delta(t) = 1$, to account for

323 complete resumption of pre-pandemic contacts (i.e., in absence of interventions and behavioral change).

324 1.7 No vaccination scenario

325 To evaluate the impact of the vaccination campaign, we need to define a suitable counterfactual scenario.

326 Simply removing vaccination from the model and letting the epidemics evolve in absence of interventions would

327 be an unrealistic scenario in terms of public health. Therefore, we chose as counterfactual a scenario where

328 governmental restrictions and individual behavior would result in the same epidemic trajectory as the one

329 observed in the presence of vaccination. We set the daily number of first doses $d_{a,c}(t)$ to 0 for all t , and

330 recalibrated at each time step the value of $\delta(t)$ necessary to match the time-series of the net reproduction

331 number estimated from surveillance data (Figure S2) [10, 24]. Then, we compared the obtained estimates of

332 social contacts, deaths, and effective reproduction number with those of the main analysis.

333

334 1.8 Future vaccination scenarios for the Delta variant

335 **Summer 2021.** We assess the combined effect of the replacement of Alpha by the Delta variant and of the

336 progression of the vaccination campaign in July and August.

337 To this aim, we estimate the reproduction number on September 7, 2021, accounting for the progression of

338 vaccination and assuming that the proportion of active pre-pandemic contacts has not changed during summer

339 2021.

340 The reproduction number can be computed through Equation 1 by:

- 341 • updating the SARS-CoV-2 immunity profile $\frac{N_a^V(t)}{N_a}$ to account for the increment in age-specific
- 342 vaccination coverage between June 30, 2021, and September 7, 2021;
- 343 • setting the proportion of active pre-pandemic contacts to the value estimated on June 30, 2021, i.e.
- 344 $\delta(t) = \delta(t^*)$ where t^* corresponds to June 30, 2021.
- 345 • adding a multiplying scale factor $(1 + \theta_{Delta})$ when assuming that the Delta variant is dominant. The
- 346 baseline value assumed for θ_{Delta} is 50% [38-40].

347 This estimate neglects the increase in natural immunity due to SARS-CoV-2 infection occurring during the

348 summer. This choice is supported by the low viral circulation in Italy in the summer, with 322,191 reported

349 cases between July 1 and September 7, 2021, corresponding to about 1.3% of the total Italian population being

350 infected after accounting for underreporting. By comparison, about 13.3% of all Italians have been fully

351 vaccinated over the same period. We also did not mechanistically model the transmission dynamics of SARS-

352 CoV-2 during the summer months because of the complexities arising from the co-circulation of two distinct

353 strains. For the purpose of our estimates, the specific dynamics of COVID-19 transmission in the summer is

354 irrelevant. In fact, the reproduction numbers estimated here only depend on the profile of population immunity

355 at the considered date.

356

357 **Future vaccination scenarios.** We provide estimates on the reproduction number to be expected for the Delta

358 variant under a set of vaccination scenarios Ω , corresponding to different improvements of the vaccination

359 coverage with respect to September 7, 2021. Vaccination scenarios Ω are defined as follows: let $Cov^*(a)$ be the

360 vaccination coverage achieved by September 7, 2021 in age group a , we define the age-specific vaccination

361 coverage in age group a under scenario Ω as:

$$362 \quad \text{Cov}(a, \Omega) = \begin{cases} 0 & \text{if } a < a_{MIN} \\ \max\{\text{Cov}^*(a), \Omega\} & \text{if } a \geq a_{MIN} \end{cases}$$

363 where a_{MIN} is the minimum age to which the vaccine is administered (12 years in the baseline analysis, 5 years
 364 when considering a pediatric vaccine). We explored values of Ω between 60% and 100% with incremental steps
 365 of 5%.

366 For each vaccination scenario Ω , we compute the reproduction number associated to different social contact
 367 levels δ^* (between 0% and 100% of pre-pandemic contacts, with incremental steps of 5%) as the dominant
 368 eigenvalue of the Next Generation Matrix defined as:

$$369 \quad NGM(\delta^*, \Omega) = \frac{\beta(1 + \theta_{Alpha})(1 + \theta_{Delta})(1 - \varphi) \delta^*}{\gamma} \begin{pmatrix} B_{a,\tilde{a}}^{V_0,IV_0}(\Omega) & B_{a,\tilde{a}}^{V_0,IV_1}(\Omega) & B_{a,\tilde{a}}^{V_0,IV_2}(\Omega) & B_{a,\tilde{a}}^{V_0,IV_3}(\Omega) & B_{a,\tilde{a}}^{V_0,IV_4}(\Omega) & B_{a,\tilde{a}}^{V_0,IV_5}(\Omega) \\ B_{a,\tilde{a}}^{V_1,IV_0}(\Omega) & B_{a,\tilde{a}}^{V_1,IV_1}(\Omega) & B_{a,\tilde{a}}^{V_1,IV_2}(\Omega) & B_{a,\tilde{a}}^{V_1,IV_3}(\Omega) & B_{a,\tilde{a}}^{V_1,IV_4}(\Omega) & B_{a,\tilde{a}}^{V_1,IV_5}(\Omega) \\ B_{a,\tilde{a}}^{V_2,IV_0}(\Omega) & B_{a,\tilde{a}}^{V_2,IV_1}(\Omega) & B_{a,\tilde{a}}^{V_2,IV_2}(\Omega) & B_{a,\tilde{a}}^{V_2,IV_3}(\Omega) & B_{a,\tilde{a}}^{V_2,IV_4}(\Omega) & B_{a,\tilde{a}}^{V_2,IV_5}(\Omega) \\ B_{a,\tilde{a}}^{V_3,IV_0}(\Omega) & B_{a,\tilde{a}}^{V_3,IV_1}(\Omega) & B_{a,\tilde{a}}^{V_3,IV_2}(\Omega) & B_{a,\tilde{a}}^{V_3,IV_3}(\Omega) & B_{a,\tilde{a}}^{V_3,IV_4}(\Omega) & B_{a,\tilde{a}}^{V_3,IV_5}(\Omega) \\ B_{a,\tilde{a}}^{V_4,IV_0}(\Omega) & B_{a,\tilde{a}}^{V_4,IV_1}(\Omega) & B_{a,\tilde{a}}^{V_4,IV_2}(\Omega) & B_{a,\tilde{a}}^{V_4,IV_3}(\Omega) & B_{a,\tilde{a}}^{V_4,IV_4}(\Omega) & B_{a,\tilde{a}}^{V_4,IV_5}(\Omega) \\ B_{a,\tilde{a}}^{V_5,IV_0}(\Omega) & B_{a,\tilde{a}}^{V_5,IV_1}(\Omega) & B_{a,\tilde{a}}^{V_5,IV_2}(\Omega) & B_{a,\tilde{a}}^{V_5,IV_3}(\Omega) & B_{a,\tilde{a}}^{V_5,IV_4}(\Omega) & B_{a,\tilde{a}}^{V_5,IV_5}(\Omega) \end{pmatrix}$$

370 where
 371

$$372 \quad B_{a,\tilde{a}}^{V_i,IV_j}(\Omega) = r_a C_{a,\tilde{a}} [1 - VE_{i,a}^{inf}] \chi_{IV_j} \frac{N_{\tilde{a}}^{V_j}(\Omega)}{N_{\tilde{a}}}$$

373 and $N_{\tilde{a}}^{V_j}(\Omega)$ represents the number of individuals of age \tilde{a} with vaccination status V_j according to vaccination
 374 scenario Ω .

375 As a baseline, we assume a transmissibility increase for the Delta variant with respect to Alpha (θ_{Delta}) equal to
 376 50% [38-40]. Alternative values of θ_{Delta} (i.e. 25% and 75%) are explored as sensitivity analyses.

377

378 2. Sensitivity analyses

379 2.1 Description

380 We assess the robustness of our results with respect to alternative assumptions on:

- 381 • the average duration of natural immunity ($1/v_R$);
- 382 • the average duration of vaccine-induced immunity ($1/v_V$);
- 383 • the relative infectiousness of SARS-CoV-2 breakthrough infections (π);
- 384 • the natural immunity level at model initialization (end of December 2020)

385 Table S2 summarizes the main model parameters and assumptions in the baseline and in alternative sensitivity
386 analyses.

387

388 **Table S2.** Description of key parameters and assumption used in the model and in alternative scenarios

Parameter description	Baseline	Alternative	Source
Epidemiological			
Generation time ($1/\gamma$)	6.6 days	-	[9]
Age-specific susceptibility to infection (r_a)	$r_a = 0.58$ (95%CI 0.34-0.98) for $a < 15$ years; $r_a = 1$ for $15 \leq a < 65$ years; $r_a = 1.65$ (95%CI 1.03-2.65) when $a \geq 65$ years	-	[4]
Duration of immunity after SARS-CoV-2 infection ($1/v_R$)	2 years	<ul style="list-style-type: none"> • 1 year • 10 years 	[7]
Age-group specific contact matrix ($C_{a,\bar{a}}$)	Contact matrix estimated for Italy before the COVID-19 pandemic	-	[3]
Initially immune individuals by age	intermediate immunity scenario (average ~15%)	<ul style="list-style-type: none"> • low immunity scenario (average ~8%) • high immunity scenario (average ~21%) 	Estimated [1] (see Section 1.3)
SARS-CoV-2 reporting ratio (ρ)	41.2%	-	Estimated (see Section 1.3)
Vaccination			
Number of doses	2	-	
Delay between 1 st dose and achievement of vaccine efficacy	14 days	-	[18]
Interval between 1 st and 2 nd dose	42 days	-	[19,20]
Delay between 2 nd dose and achievement of vaccine efficacy	7 days	-	[18]
Efficacy against infection immediately after 1 st dose ($VE_{1,a}^{inf}$)	0% for all ages	-	
Full efficacy against infection of 1 st dose ($VE_{2,a}^{inf}$)	Age-specific: average 75.5% (range 70.6%-78.8%)	-	Estimated (see Section 1.5)
Efficacy against infection immediately after 2 nd dose ($VE_{3,a}^{inf}$)	Same as $VE_{2,a}$	-	Assumed
Full efficacy against infection of 2 nd dose ($VE_{4,a}$)	Age-specific: average 88.7% (range 79.4%-88.7 %) - see Section 1.5	-	Estimated (see Section 1.5)
Efficacy against infection after waning of vaccine protection ($VE_{5,a}$)	0% for all ages	-	Assumed
Relative infectiousness of SARS-CoV-2 breakthrough infections (π)	50%	100%	[5,6]
Duration of vaccine protection ($1/v_V$)	2 years	<ul style="list-style-type: none"> • 1 year • 10 years 	[8]

389

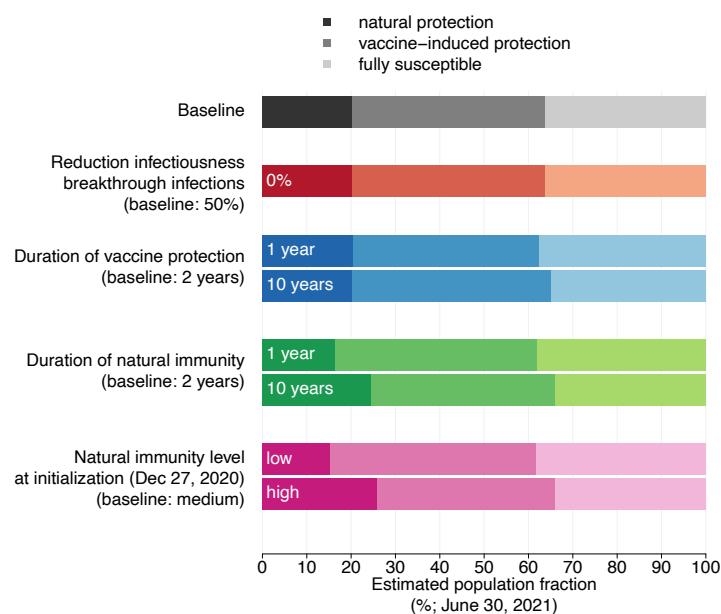
390

391 **2.2 Results**

392 Figure S8-S10 shows that model results are most sensitive to the duration of natural immunity and the initial
 393 immunity profile, but that overall the estimates are quite robust. In particular, the estimate for June 30, 2021 of
 394 the average proportion of fully susceptible individuals ranges between 34% and 38% (Figure S8), that of social
 395 contacts ranges between 44% and 53% of pre-pandemic contacts (Figure S9) and that of the effective
 396 reproduction number ranges between 1.7 and 2.1 (Figure S10).

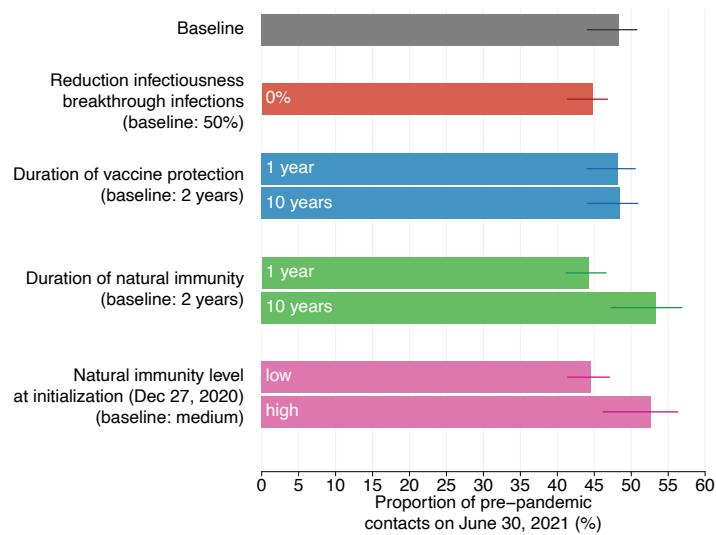
397 Results obtained for future vaccination scenarios suggest that, if the vaccine did not reduce the infectiousness
 398 of breakthrough infections, the social contact levels that could be achieved without causing an epidemic would
 399 be about 45-65% (depending on the coverage scenario) compared to 55%-70% for the baseline (Figure S11).

400 The duration of vaccine-induced protection affects very marginally results for the prospective vaccination
 401 scenarios (Figure S12), due to the fact that the majority of vaccines have been administered too recently for
 402 waning to have a major effect. On the other hand, shorter duration of natural immunity, or a lower level of
 403 natural immunity at model initialization, would result in a slightly lower level of social contacts that could be
 404 resumed without causing an epidemic (namely, 50-70% for a duration of immunity of 1 year and 50-70% for an
 405 initial immunity profile that is lower than estimated - see Figures S13-S14, left panels).

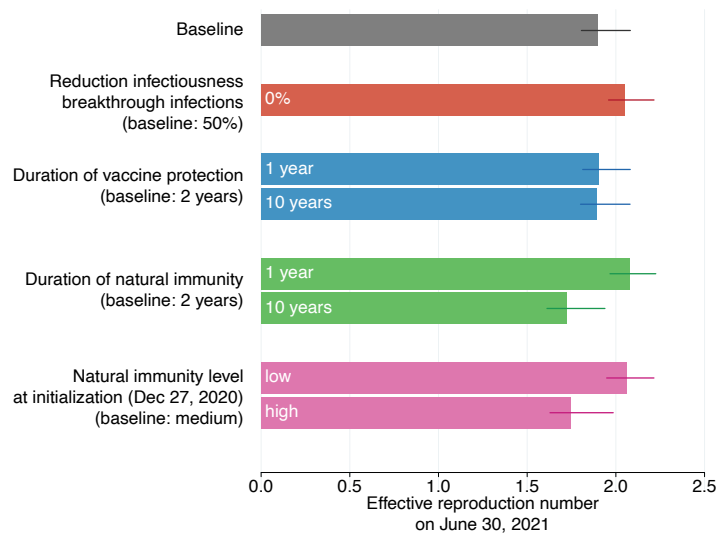


406

407 **Figure S8.** Estimated immunity profile of the overall Italian population on June 30, 2021 for the baseline analysis and for the
 408 sensitivity analyses considered. Individuals who have been infected after being vaccinated or who have been vaccinated
 409 despite still having a protection from infection are counted under the natural protection bar; individuals who have never
 410 been infected or who have lost their natural protection and were vaccinated (partially or fully) are included under the
 411 vaccine-induced protection bar; individuals who were never vaccinated nor infected, or who were infected but lost their
 412 natural protection, or who were vaccinated but lost their vaccine-induced protection are included under the fully susceptible
 413 bar.

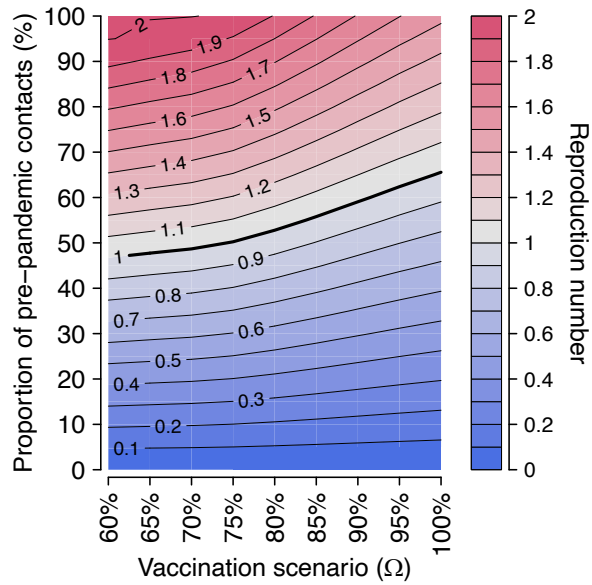


414 **Figure S9.** Estimated active social contacts on June 30, 2021, as a proportion of pre-pandemic contacts for the baseline
 415 analysis and for the sensitivity analyses considered. Bars: mean estimates; horizontal lines: 95% CI.
 416

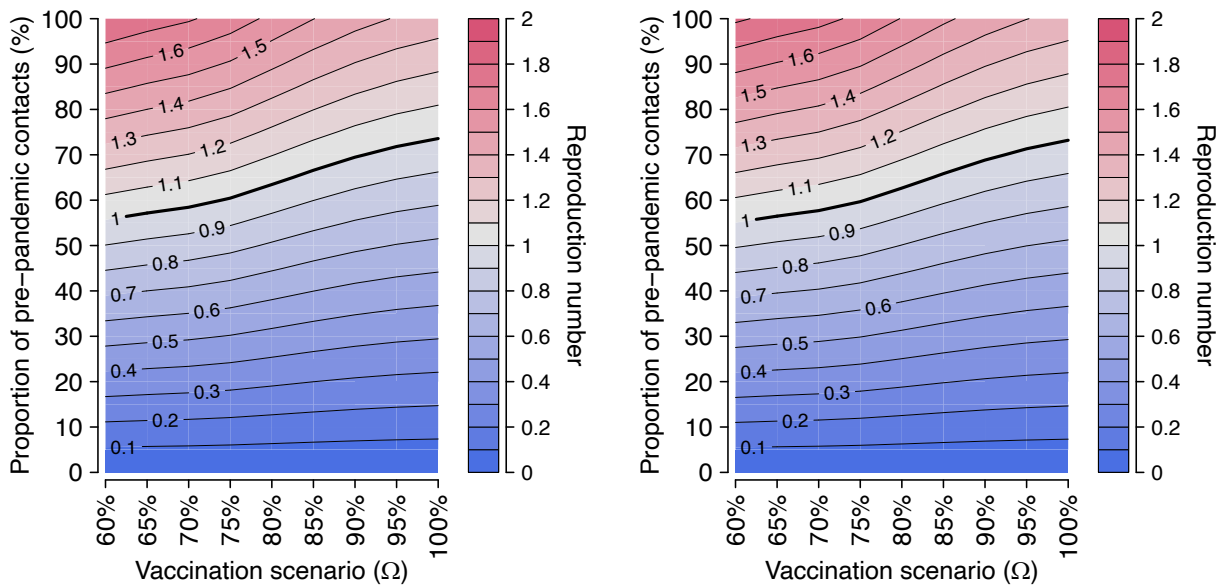


417 **Figure S10.** Effective reproduction number (i.e., under complete resumption of pre-pandemic contacts) on June 30, 2021 for
 418 the baseline analysis and for the sensitivity analyses considered. Bars: mean estimates; horizontal lines: 95% CI.
 419
 420

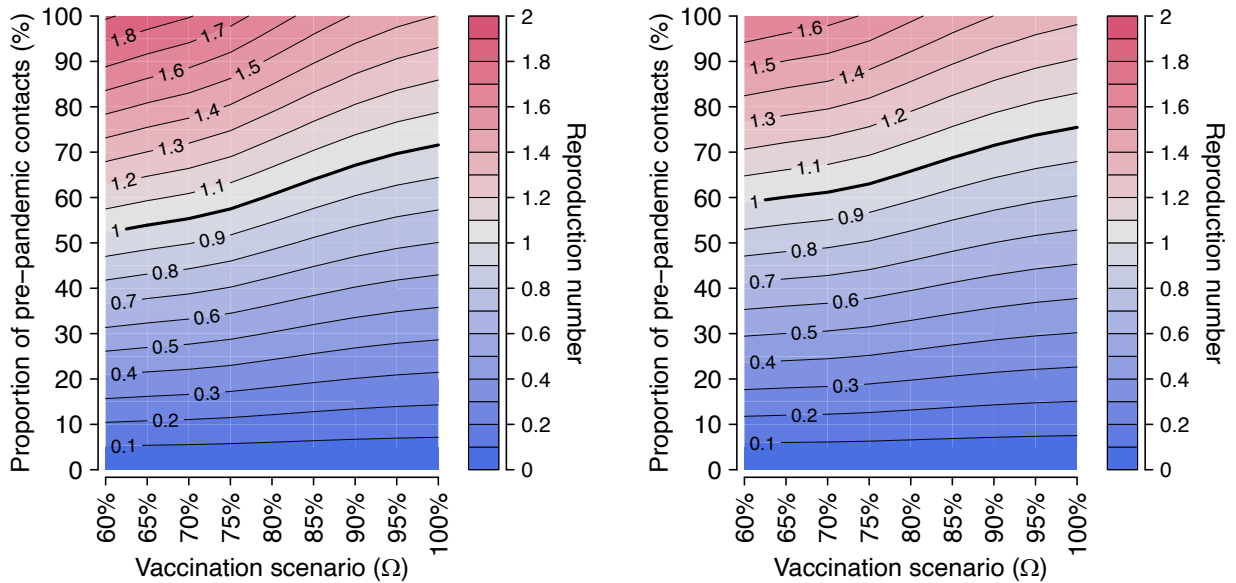
421
 422
 423



424
 425 **Figure S11. Sensitivity analysis with respect to the relative infectiousness of SARS-CoV-2 breakthrough infections ($\pi=100\%$).**
 426 Heatmap of the estimated reproduction number for different vaccination scenarios (x axis) and different levels of social
 427 activity (y axis). Contour lines discriminate different values of the reproduction number. The thicker contour line represents
 428 the epidemic threshold of 1.
 429

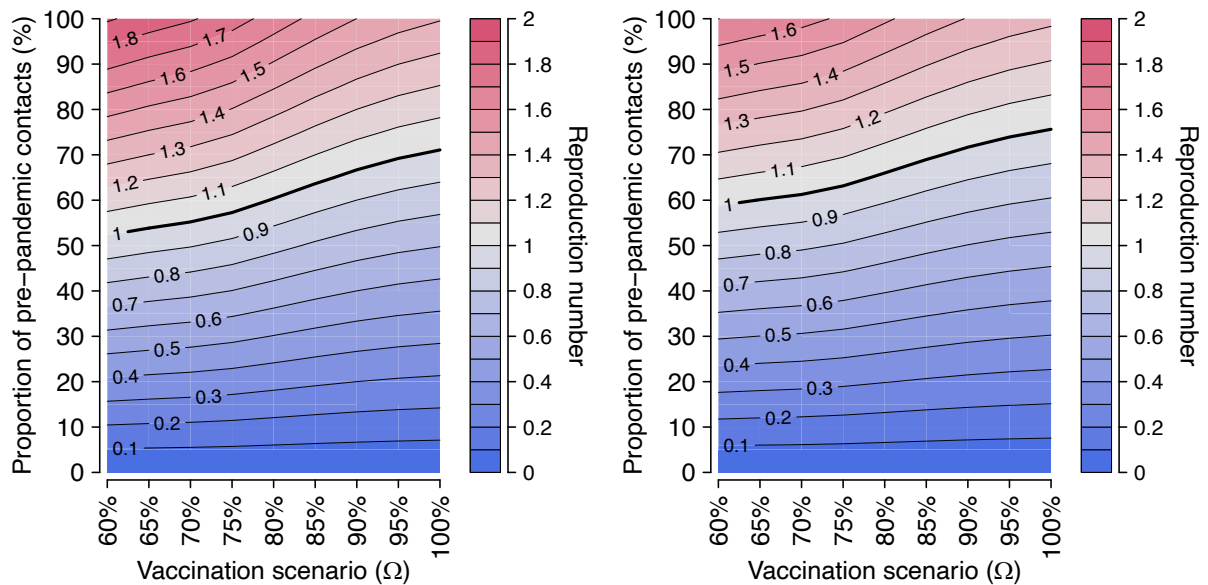


430 **Figure S12. Sensitivity analysis with respect to the duration of vaccine-induced immunity ($1/v_V$).** Heatmap of the estimated
 431 reproduction number for different vaccination scenarios (x axis) and different levels of social activity (y axis), under different
 432 average durations of vaccine protection: 1 year (left) and 10 years (right)



433
434
435
436

Figure S13. Sensitivity analysis with respect to the duration of natural immunity ($1/v_R$). Heatmap of the estimated reproduction number for different vaccination scenarios (x axis) and different levels of social activity (y axis), under different average durations of natural immunity: 1 year (left) and 10 years (right).



437
438
439
440
441
442

Figure S14. Sensitivity analysis with respect to the level of initial immunity. Heatmap of the estimated reproduction number for different vaccination scenarios (x axis) and different levels of social activity (y axis), under different initial levels of natural immunity: low immunity scenario (left) and high immunity scenario (right).

443 References

- 444 1. Marziano, V. et al. Retrospective analysis of the Italian exit strategy from COVID-19 lockdown. Proc.
445 Natl Acad. Sci. 118, e2019617118 (2021).
- 446 2. Yang, J. et al. Despite vaccination, China needs non-pharmaceutical interventions to prevent
447 widespread outbreaks of COVID-19 in 2021. Nat. Hum. Behav. 5, 1009–1020 (2021).
- 448 3. Mossong, J. et al. Social contacts and mixing patterns relevant to the spread of infectious diseases.
449 PLoS Med. 5, e74 (2008).
- 450 4. Hu, S. et al. Infectivity, susceptibility, and risk factors associated with SARS-CoV-2 transmission under
451 intensive contact tracing in Hunan, China. Nat. Commun. 12, 1533 (2021).

- 452 5. Harris, R.J., Hall, J.A., Zaidi, A., Andrews, N.J., Dunbar, J. K., Dabrera, G. Effect of Vaccination on
453 Household Transmission of SARS-CoV-2 in England. *N. Engl. J. Med.* 385(8):759-760. doi:
454 10.1056/NEJMc2107717 (2021).
- 455 6. Lipsitch, M. & Kahn, R. Interpreting vaccine efficacy trial results for infection and transmission. *Vaccine*,
456 39(30): 4082-4088 (2021).
- 457 7. Hall, V. J. et al. SARS-CoV-2 infection rates of antibody-positive compared with antibody-negative
458 health-care workers in England: a large, multicentre, prospective cohort study (SIREN). *Lancet* 397,
459 1459–1469 (2021).
- 460 8. Andrews, N. Vaccine effectiveness and duration of protection of Comirnaty, Vaxzevria and Spikevax
461 against mild and severe COVID-19 in the UK. medRxiv. doi:
462 <https://doi.org/10.1101/2021.09.15.21263583> (2021).
- 463 9. Cereda, D. et al. The early phase of the COVID-19 outbreak in Lombardy, Italy.
464 <https://arxiv.org/pdf/2003.09320.pdf> (2020).
- 465 10. Riccardo, F. et al. Epidemiological characteristics of COVID-19 cases and estimates of the reproductive
466 numbers 1 month into the epidemic, Italy, 28 January to 31 March 2020. *Eurosurveillance* 25, 2000790
467 (2020).
- 468 11. Guzzetta, G. et al. Impact of a nationwide lockdown on sars-cov-2 transmissibility, Italy. *Emerg. Infect.*
469 *Dis.* 27, 267 (2021).
- 470 12. Stefanelli P. et al. Co-circulation of SARS-CoV-2 Alpha and Gamma variants in Italy, February-March
471 2021. *Eurosurveillance* (in press).
- 472 13. Volz, E. et al. Assessing transmissibility of SARS-CoV-2 lineage B.1.1.7 in England. *Nature* 593, 266–269
473 (2021).
- 474 14. Davies, N. G. et al. Estimated transmissibility and impact of SARS-CoV-2 lineage B.1.1.7 in England.
475 *Science* <https://doi.org/10.1126/science.abg3055> (2021).
- 476 15. Gaymard, A. et al. Early assessment of diffusion and possible expansion of SARS-CoV-2 Lineage
477 20I/501Y. V1 (B. 1.1. 7, variant of concern 202012/01) in France, January to March 2021.
478 *Eurosurveillance*, 26(9):2100133 (2021).
- 479 16. Galloway, S. E. et al. Emergence of SARS-CoV-2 B.1.1.7 lineage—United States, December 29, 2020 –
480 January 12, 2021. *Morbidity and Mortality Weekly Report*. 2021 Jan 22;70(3):95.
- 481 17. Struttura Commissariale per l’Emergenza Covid-19. Open data on COVID-19 vaccination in Italy.
482 <https://github.com/italia/covid19-opendata-vaccini>. Accessed on October 15, 2021
- 483 18. Dagan N, Barda N, Kepten E, Miron O, Perchik S, Katz MA, et al. BNT162b2 mRNA Covid-19 vaccine in a
484 nationwide mass vaccination setting. *N Engl J Med*. 2021 Feb 24.
485 <https://doi.org/10.1056/NEJMoa2101765>.
- 486 19. Trasmissione parere del CTS in merito alla estensione dell’intervallo tra le due dosi dei vaccini a mRNA
487 e alla seconda dose del vaccino Vaxzevria. Available at:
488 [https://www.trovanorme.salute.gov.it/norme/renderNormsanPdf?anno=2021&codLeg=80236&parte=](https://www.trovanorme.salute.gov.it/norme/renderNormsanPdf?anno=2021&codLeg=80236&parte=1%20&serie=null)
489 [1%20&serie=null](https://www.trovanorme.salute.gov.it/norme/renderNormsanPdf?anno=2021&codLeg=80236&parte=1%20&serie=null).
- 490 20. Joint Committee on Vaccination and Immunisation (UK). Optimising the COVID-19 vaccination
491 programme for maximum short-term impact. Available at:
492 [https://www.gov.uk/government/publications/prioritising-the-first-covid-19-vaccine-dose-jcvi-](https://www.gov.uk/government/publications/prioritising-the-first-covid-19-vaccine-dose-jcvi-statement/optimising-the-covid-19-vaccination-programme-for-maximum-short-term-impact)
493 [statement/optimising-the-covid-19-vaccination-programme-for-maximum-short-term-impact](https://www.gov.uk/government/publications/prioritising-the-first-covid-19-vaccine-dose-jcvi-statement/optimising-the-covid-19-vaccination-programme-for-maximum-short-term-impact).
- 494 21. Diekmann, O., Heesterbeek, J. A. P. & Metz, J. A. On the definition and the computation of the basic
495 reproduction ratio R_0 in models for infectious diseases in heterogeneous populations. *J. Math Biol.* 28,
496 365–382 (1990).
- 497 22. Diekmann, O., Heesterbeek, J. A. & Roberts, M. G. The construction of next-generation matrices for
498 compartmental epidemic models. *J. R. Soc. Interface* 7, 873–885 (2010).
- 499 23. Marziano, V., Poletti, P., Trentini, F., Melegaro, A., Ajelli, M. & Merler, S. Parental vaccination to reduce
500 measles immunity gaps in Italy. *Elife*. 2019 Sep 3;8:e44942.

- 501 24. Istituto Superiore di Sanità. Epidemia COVID-19 - Aggiornamento nazionale 6 ottobre 2021. Available
502 at: [https://www.epicentro.iss.it/coronavirus/bollettino/Bollettino-sorveglianza-integrata-COVID-19_6-](https://www.epicentro.iss.it/coronavirus/bollettino/Bollettino-sorveglianza-integrata-COVID-19_6-ottobre-2021.pdf)
503 [ottobre-2021.pdf](https://www.epicentro.iss.it/coronavirus/bollettino/Bollettino-sorveglianza-integrata-COVID-19_6-ottobre-2021.pdf)
- 504 25. Italian National Institute of Statistics. Popolazione residente per età, sesso e stato civile al 1 Gennaio
505 2020. <http://demo.istat.it/pop2020/index.html>. Accessed March 15, 2021.
- 506 26. Italian National Institute of Statistics. Indagine Multiscopo sulle famiglie: aspetti della vita quotidiana.
507 <http://dati.istat.it/Index.aspx?QueryId=15448#> [Italian] Accessed March 15, 2021.
- 508 27. Istituto Superiore di Sanità. COVID-19 ISS open data – EpiCentro. Available at:
509 https://www.epicentro.iss.it/coronavirus/open-data/covid_19-iss.xlsx. Accessed on October 15, 2021
- 510 28. Poletti, P. et al. Age-specific SARS-CoV-2 infection fatality ratio and associated risk factors, Italy,
511 February to April 2020. *Eurosurveillance* 2020 Aug 6;25(31):2001383.
- 512 29. Trentini, F. et al. The pressure on healthcare system and intensive care utilization during the COVID-19
513 outbreak in the Lombardy region: a retrospective observational study on 43,538 hospitalized patients.
514 *Am. J. Epidemiol.* doi: 10.1093/aje/kwab252
- 515 30. Dipartimento di Protezione Civile, COVID-19 Italia - Monitoraggio situazione. [https://github.com/pcm-](https://github.com/pcm-dpc/COVID-19)
516 [dpc/COVID-19](https://github.com/pcm-dpc/COVID-19). Accessed March 15, 2021.
- 517 31. WHO SAGE roadmap for prioritizing uses of COVID-19 vaccines in the context of limited supply.
518 [https://www.who.int/docs/default-source/immunization/sage/covid/sage-prioritization-roadmap-](https://www.who.int/docs/default-source/immunization/sage/covid/sage-prioritization-roadmap-covid19-vaccines.pdf?Status=Temp&sfvrsn=bf227443_2)
519 [covid19-vaccines.pdf?Status=Temp&sfvrsn=bf227443_2](https://www.who.int/docs/default-source/immunization/sage/covid/sage-prioritization-roadmap-covid19-vaccines.pdf?Status=Temp&sfvrsn=bf227443_2). Accessed March 15, 2021.
- 520 32. Ministry of Health. Raccomandazioni ad interim sui gruppi target della vaccinazione anti SARS-CoV-
521 2/COVID-19. Available at:
522 [https://www.trovanorme.salute.gov.it/norme/renderPdf.spring?seriegu=SG&datagu=24/03/2021&red](https://www.trovanorme.salute.gov.it/norme/renderPdf.spring?seriegu=SG&datagu=24/03/2021&redaz=21A01802&artp=1&art=1&subart=1&subart1=10&vers=1&prog=002)
523 [az=21A01802&artp=1&art=1&subart=1&subart1=10&vers=1&prog=002](https://www.trovanorme.salute.gov.it/norme/renderPdf.spring?seriegu=SG&datagu=24/03/2021&redaz=21A01802&artp=1&art=1&subart=1&subart1=10&vers=1&prog=002)
- 524 33. Emary, K. R. W. et al. Efficacy of ChAdOx1 nCoV-19 (AZD1222) vaccine against SARS-CoV-2 variant of
525 concern 202012/01 (B.1.1.7): an exploratory analysis of a randomised controlled trial. *Lancet*,
526 397(10282), 1351-1362 (2021).
- 527 34. Abu-Raddad, L. J., Chemaitelly, H., Butt, A. A. & National Study Group for COVID-19 Vaccination.
528 Effectiveness of the BNT162b2 Covid-19 Vaccine against the B.1.1.7 and B.1.351 Variants. *N. Engl. J.*
529 *Med.*, 385(2):187-189. doi: 10.1056/NEJMc2104974 (2021).
- 530 35. Shapiro, J., Dean, N. E., Madewell, Z. J., Yang, Y., Halloran, M. E., Longini, I. Efficacy Estimates for
531 Various COVID-19 Vaccines: What we Know from the Literature and Reports. medRxiv. doi:
532 <https://doi.org/10.1101/2021.05.20.21257461> (2021).
- 533 36. Thompson, M. G. et al. Interim estimates of vaccine effectiveness of BNT162b2 and mRNA-1273
534 COVID-19 vaccines in preventing SARS-CoV-2 infection among health care personnel, first responders,
535 and other essential and frontline workers — eight U.S. locations, December 2020–March 2021. *MMWR*
536 70, 495–500 (2021).
- 537 37. Istituto Superiore di Sanità. Epidemia COVID-19 - Aggiornamento nazionale 28 luglio 2021. Available
538 at: [https://www.epicentro.iss.it/coronavirus/bollettino/Bollettino-sorveglianza-integrata-COVID-19_28-](https://www.epicentro.iss.it/coronavirus/bollettino/Bollettino-sorveglianza-integrata-COVID-19_28-luglio-2021.pdf)
539 [luglio-2021.pdf](https://www.epicentro.iss.it/coronavirus/bollettino/Bollettino-sorveglianza-integrata-COVID-19_28-luglio-2021.pdf)
- 540 38. Campbell, F. et al. Increased transmissibility and global spread of SARS-CoV-2 variants of concern as at
541 June 2021. *Eurosurveillance* 26(24):2100509. doi: 10.2807/1560-7917.ES.2021.26.24.2100509 (2021).
- 542 39. Keeling, M. J. Estimating the Transmission Advantage for B.1.617.2. Available at:
543 [https://assets.publishing.service.gov.uk/government/uploads/system/uploads/attachment_data/file/9](https://assets.publishing.service.gov.uk/government/uploads/system/uploads/attachment_data/file/993156/S1269_WARWICKTransmission_Advantage.pdf)
544 [93156/S1269_WARWICKTransmission_Advantage.pdf](https://assets.publishing.service.gov.uk/government/uploads/system/uploads/attachment_data/file/993156/S1269_WARWICKTransmission_Advantage.pdf)
- 545 40. Alizon, S. et al. Rapid spread of the SARS-CoV-2 Delta variant in some French regions, June 2021.
546 *Eurosurveillance*, 26(28): 2100573 (2021).

547
548
549
550
551